Predicting tropical tree mortality with leaf spectroscopy

Predicting tropical tree mortality with leaf spectroscopy

Authors: Christopher E. Doughty*[1], Alexander W. Cheesman[2,3], Terhi Riutta[4,5], Eleanor Thomson[4], Alexander Shenkin[4], Andrew T. Nottingham[6,7], Elizabeth M. Telford[7], Walter Huaraca Huasco[4], Noreen Majalap[8], Yit Arn Teh[9], Patrick Meir[10,7], Yadvinder Malhi[4]

Affiliations:

[1]*School of Informatics, Computing, and Cyber Systems, Northern Arizona University, Flagstaff, AZ. 86011, USA*

2 College of Life and Environmental Sciences, University of Exeter, Exeter, Devon EX4 4QF, United Kingdom

3 College of Science & Engineering, James Cook University, Cairns, Queensland 4870, Australia

4 Environmental Change Institute, School of Geography and the Environment, University of Oxford, Oxford OX1 3QY, United Kingdom

5 Imperial College London, Department of Life Sciences, Silwood Park Campus, Buckhurst Road, Ascot, SL5 7PY, UK

6 Smithsonian Tropical Research Institute, 0843-03092, Balboa, Ancon, Republic of Panama

7 School of Geosciences, University of Edinburgh, Crew Building, Kings Buildings, Edinburgh EH9 3FF, United Kingdom

8 Forest Research Centre, Sabah Forestry Department, 90715 Sandakan, Sabah, Malaysia.

9 Newcastle University, School of Natural and Environmental Sciences, Newcastle Upon Tyne, NE1 7RU, UK

10 Research School of Biology, Australian National University, ACT 2602 Australia

Abstract – Do tropical trees close to death have a distinct change to their leaf spectral signature? Tree mortality rates have been increasing in tropical forests globally, reducing the global carbon sink. Upcoming hyperspectral satellites could be used to predict regions close to experiencing extensive tree mortality during periods of stress, such as drought. Here we show, for a tropical rainforest in Borneo, how imminent tropical tree mortality impacts leaf physiological traits and reflectance. We measured leaf reflectance (400-2500 nm), light saturated photosynthesis (A_{sat}), leaf dark respiration (R_{dark}), leaf mass area (LMA) and % leaf water across five campaigns in a six-month period during which there were two causes of tree mortality: a major natural drought and a co-incident tree stem girdling treatment. We find that prior to mortality, there were significant ($P<0.05$) leaf spectral changes in the red (650-700 nm), the NIR (1000 -1400 nm) and SWIR bands (2000-2400 nm) and significant reductions in the potential carbon balance of the leaves (increased R_{dark} and reduced A_{sat}). We show that the partial least squares regression technique can predict mortality in tropical trees across different species and functional groups with medium precision but low accuracy (r^2 of 0.65 and RMSE/mean of 0.58). However, most tree death in our study was due to girdling, which is not a natural form of death. More research is needed to determine if this spectroscopy technique can be applied to tropical forests in general.

Keywords – Tropical forests, spectroscopy, girdling, tree mortality, traits, drought, el Niño

Introduction

Can future tropical forest tree mortality be predicted with aircraft or satellite remote sensing? This question is of interest because tropical tree mortality is increasing, reducing the global carbon sink (Brienen et al., 2015; Hubau et al., 2020). Increased tree mortality may be driven by recent increases in extreme weather events caused by climate change, including increased drought frequency/severity (Doughty et al., 2015; Rifai et al., 2018, 2019; Rowland et al., 2015) or elevated air temperatures (Clark, 2004; Doughty & Goulden, 2009a). Other causes of mortality include altered disturbance regimes due to land management practices or biological invasions (e.g. grass/fire cycles) and the negative environmental impacts arising from forest degradation (e.g. physical damage to trees from logging or small-scale slash-and-burn agriculture; environmental stress from enhanced edges effects) (Malhi et al., 2014). Experimental drought manipulations in the Amazon (da Costa et al., 2010; Meir et al., 2015; Nepstad et al., 2007) show that larger trees are more susceptible to drought-related mortality for specific high-abundance taxa (Bittencourt et al., 2020).

Could changes to leaf properties in these large trees indicate risk of imminent future mortality? Death of these large individuals has the greatest impact on tropical forest vegetation and carbon dynamics (Phillips et al., 2009). "Environmental surveillance" techniques that enable us to identify individuals at risk of mortality or to predict future patterns of senescence would enable us not only to model forest vegetation and carbon dynamics more accurately, but could possibly enable us to manage the spread of forest pathogens and understand environmental stress gradients related to disturbance. Given that these large trees are also the most visible to aircraft and satellites, remote sensing techniques that enable us to identify dying trees hold

68 tremendous potential for detecting and understanding the causes of tree mortality at large spatial
69 scales.

70 Leaf traits, such as leaf chemical composition, photosynthetic capacity or leaf mass per
71 area (LMA), are important indicators of a tree's life history strategy and overall vitality (Poorter
72 et al., 2008; Wright et al., 2004; Wright et al., 2010). Remote sensing of these traits is thus one
73 approach that could enable us to detect individuals or taxa at elevated risk of death from stress.
74 For instance, light-demanding species with rapid growth and high mortality rates are predicted to
75 have lower seed mass, leaf mass per area (LMA), wood density, and tree height (Wright et al.,
76 2010). Variation in LMA in part expresses a trade-off between the energetic cost of leaf
77 construction and the light captured per area that may be reflective of the strategy of the broader
78 tree itself (Díaz et al., 2016; Poorter et al., 2009). Drought tolerance is also reflected in structural
79 traits such as LMA, leaf thickness, leaf toughness and wood density, although further studies are
80 required to better establish the limitations of these metrics and identify other potential indices
81 (Bartlett et al., 2012; Fyllas et al., 2012; Niinemets, 2001; Zanne et al., 2010).

82 Much recent literature has discussed the roles of carbon starvation, hydraulic failure, or a
83 combination of the two on tree death as well as the traits associated with these processes. To
84 predict tree death with remote sensing we must first understand the characteristics that drive tree
85 death. A recent meta-analysis suggests that metrics of hydraulic failure more consistently
86 predicted mortality than carbon starvation as determined by tissue concentrations of non-
87 structural carbohydrates (NSC) (Adams et al., 2017). Another study similarly found hydraulic
88 traits were better at predicting the response of ecosystem fluxes (CO_2 and water vapor) to
89 drought than traits like LMA or wood density (Anderegg et al., 2018). Tree mortality during
90 droughts is highest for species that have a small hydraulic safety margin (the difference between

typical minimum xylem water potential experienced and xylem vulnerability to embolism) (Anderegg et al., 2016). Turgor loss point - the leaf water potential that induces wilting - may be a key trait predicting drought tolerance and species distributions relative to water supply (Bartlett et al., 2012). In tropical forests, turgor loss point varied widely across species and was weakly positively correlated with leaf toughness and thickness (Maréchaux et al., 2015). Some literature suggests that both hydraulic failure and carbon depletion are associated with mortality in large part through their effect on leaf water content and turgor (Sapes et al., 2019; Sevanto et al., 2014). Leaf water content can be accurately remotely sensed at the leaf and aircraft scale (Asner et al., 2016; Asner & Martin, 2008).

Leaf traits can be sensed remotely by aircraft or from space. Foliar traits such as nitrogen (N) content, chlorophyll content, carotenoids, lignin, cellulose, LMA, soluble carbon, and water can be remotely estimated with leaf spectral reflectance signatures (400-2500nm in 1 nm bandwidths) in many different plants and ecosystems (Ustin et al., 2009), including tropical forests (Asner & Martin, 2008). This is because certain traits are associated with reflectance characteristics within specific spectral regions. For instance, the visible part of the spectrum (400–700 nm) is associated with pigments (mostly chlorophyll), and the near infrared (NIR; 700–1,300 nm) is associated with structures such as palisade cell density. LMA and leaf chemistry have been accurately measured and modelled at both the leaf (Asner & Martin, 2008; Curran, 1989; Jacquemoud et al., 2009), canopy and landscape scales (Asner et al., 2016). Other elements not directly expressed in the spectrum, such as phosphorus (P), have been accurately predicted with spectroscopy, possibly through stoichiometric relationships with other chemical species (Ustin et al., 2006, 2009) or correlations with leaf morphological traits via the leaf economics spectrum (Wright et al 2004). Other tropical tree traits not directly associated with

leaf spectra, such as photosynthetic capacity (Doughty et al., 2011), and branch wood density, have been predicted with spectroscopy in tropical forests (Doughty et al., 2017). Traits not directly associated with spectral regions can still be predicted through correlations between leaf traits and a tree's life history strategy (Doughty et al., 2017).

There is evidence that drought changes tropical forest reflectance at the continental scale, due to changes in leaf traits or increased tree mortality. For instance, Enhanced Vegetation Index (EVI), a greenness index measured with Moderate Resolution Imaging Spectroradiometer (MODIS), increased in the Amazon during the 2005 drought, indicating possible positive impacts of drought on forests due to increased irradiance (Saleska et al., 2007). However, others have challenged the original interpretation of the EVI data (Morton et al., 2014; Samanta et al., 2010), highlighting the challenge of remote sensing at a continental scale. More recently, during a major El Niño drought in Borneo, NDVI initially increased as the drought was strengthening, but decreased at its peak (Nunes et al., 2019). Interpretation of changing NDVI and/or EVI at larger spatial scales is generally complicated in many ecosystems as changes at the leaf level may be compensated for or masked by canopy scale process. For example, leaf senescence and leaf fall may reduce the canopy scale NIR signal. However, remotely sensed LAI signal saturates in tropical forests and LAI variation can be relatively small even following strong climate extremes such as drought. For instance, Meir et al. (2018) found a 12-20% change in LAI during an extreme drought manipulation experiment with a non-droughted natural LAI of ~5.5 m^2 m^{-2}, which is within the saturation range. Therefore, changes in tropical forest canopy spectral characteristics at larger spatial scales may be more linked to changes in leaf level spectra, than in other ecosystems with lower LAI (Doughty & Goulden, 2009b; Wu et al., 2018).

The 2016 El Niño caused a significant drought in Borneo, both in terms of increased maximum temperatures and reduced precipitation (Figure 1)(Rifai et al., 2019)(Rifai et al., 2018). This El Niño had unusually high temperatures, which have been attributed to climate change (Thirumalai et al., 2017). Recent work in Borneo, near our study site, found the El Niño event was associated with a decrease in chlorophyll and carotenoid concentrations by 35%. They also noted a decrease in NDVI with a change in the shortwave infrared region of leaf spectral signatures (Nunes et al., 2019). The authors hypothesized that trees produced new leaves with higher pigment concentrations at the start of the El Niño event, and then dropped their leaves at its peak.

In this study, we focus on tree mortality at a 1 ha long-term study site close to the Nunes et al (2019) study site in Sabah, northern Borneo. We attempt to understand the relationship between leaf traits, spectroscopy and mortality in two different ways: natural death during El Niño and forced mortality induced by girdling. Before, during and after the 2016 El Niño drought (over 5 field campaigns), we measured canopy-top leaf spectra (400-2500 nm), net light saturated photosynthesis, dark respiration and LMA in a representative cross section of the 393 monitored trees. We further tried to explore mechanisms of mortality with a girdling campaign (the removal of the phloem in a 10 cm ring around the tree stem) in one half (0.5 ha, 210 stems) of the plot. Here, we test the following hypotheses:

H1 – Leaf traits that are correlated with leaf spectroscopy signals, such as light saturated photosynthesis, dark respiration, and LMA, undergo significant change months prior to tree mortality.

H2 - Tropical tree mortality can be predicted with hyperspectral information (400-2500 at 1 nm bandwidth leaf reflectance).

Methods

Study sites

Our study plots are in Kalabakan Forest Reserve in Sabah, Malaysian Borneo (Tower SAF-05 4.716°, 117.609°) within the Stability of Altered Forest Ecosystems (SAFE) Project study site (Ewers et al., 2011; Riutta et al., 2018). A schematic of the study site is shown in figure 1C. Mean annual temperature is approximately 26.7°C and mean annual precipitation is 2,600–2,700 mm with no distinct dry season but, on average, ~12% of months with precipitation below 100 mm $month^{-1}$ (Walsh & Newbery, 1999). The plot has been selectively logged four times since the 1970s, which represents a high logging intensity for this region. The soils are orthic Acrisols or Ultisols on undulating clay soil. The tree basal area is 13.9 m^2/ha. Total NPP and autotrophic respiration have been measured at this plot since 2011 and there is an eddy covariance tower nearby (Riutta et al., 2018). The plot is split in half by a small stream. All the trees on one side of the stream were girdled in late January 2016 by removing the phloem tissue in a 10 cm band, as described below (note: the plot was in the process of conversion to oil palm agriculture production). This part of the study site is hereafter referred to as the "girdled plot." The trees on the other side of the stream were not girdled and represent the treatment control. This part of the study site is hereafter referred to as the "drought plot". Although all trees experienced drought, the "drought" plot only experienced drought and not the effects of girdling. We collected data during five field campaigns that took place from January to June 2016. Campaigns began on the following days and generally took several days: Campaign 1=21 Jan-16, Campaign 2=10 Feb-16, Campaign 3=01 Mar-16, Campaign 4=29 Mar-16, Campaign 5 08 Jun-16. The first field campaign (C1) was conducted before girdling occurred to determine pre-girdling conditions and process rates.

Girdling experiment – In late Jan 2016, after the first field campaign, we further explored the causes of tree mortality by conducting a girdling experiment. Girdling involved removing a 10 cm strip of the periderm and phloem in a ring around the tree stem at ~1.2 m height (with exceptions for trees with buttresses, which were girdled above the buttress) above the soil (Figure 1a) in a plot that was scheduled for conversion to a palm oil plantation. This technique prevents carbohydrate transport to the roots but maintains hydraulic connectivity because xylem tissues are not severed. Tree death was determined visually, based on the absence of visible canopy, with regular (average 18-day period) visits to the plots for both the drought and the girdled plots. We give the species measured in both plots in Table 1.

Leaf sampling strategy –In each plot, 20-25 trees were chosen during each campaign, and tree climbers with extendable tree pruners removed one branch per tree that was growing in full sunlight (Asner & Martin, 2008). These branches were quickly recut underwater and taken to the laboratory for further measurements. On each of these branches, five fully expanded non-senescent leaves in randomly selected locations were chosen for measurements of: leaf-gas exchange leaf spectral properties (measured within 1 hour of being cut) and LMA. Leaf area was determined immediately after collection using a digital 476 scanner (Canon LiDE 110). Leaves were then oven dried at 72 °C until constant mass was reached. We subtracted wet weight from dry weight to calculate % leaf water and used dry weight and leaf area in order to calculate LMA.

Leaf-level gas exchange – We used a portable gas exchange system (LI 6400, Li-Cor Biosciences, Lincoln, NE, USA) to measure leaf-level gas exchange. After returning to the laboratory, leaf dark respiration (R_{dark}) was measured by covering branches with an opaque bag for at least 20 minutes prior to measurement at a cuvette temperature of 30° C (Rowland et al., 2017). After this, branches were exposed to sunlight and light-saturated leaf photosynthesis was measured (A_{sat}; 1200 μmol m^{-2} s^{-1} PPFD, 400 ppm CO_2, at 30° C). We chose a light level of 1200 μmol m^{-2} s^{-1} for A_{sat} because we tested photosynthetic capacity and found it generally saturated below light levels of ~1200 μmol m^{-2} s^{-1} PPFD, similar to other tropical studies (Both et al., 2019; Gvozdevaite et al., 2018; Doughty & Goulden, 2009b). We waited for gas exchange values to stabilize before starting a measurement, recorded data every two seconds and averaged the results after eliminating the first 20 measurements. We excluded photosynthesis measurements less than 0 μmol m^{-2} s^{-1} as this was indicative of a failure to maintain hydraulic connectivity in the sampled branch resulting in stomatal closure. We also excluded dark respiration measurements more negative than -1.5 μmol m^{-2} s^{-1} as this was considered indicative of a failure to truly represent $R_{d,}$ or in some cases operator error. Most physiological measurements were collected between 07:00 and 14:00 local time and branches were cut from trees between 06:00 and 13:00 local time. An online supplement includes our averaged ± sd data for each leaf measured for transpiration rate (mmol H_2O m^{-2} s^{-1}), vapor pressure deficit based on leaf temperature (kPa), intercellular CO_2 concentration (μmol CO_2 mol^{-1}), conductance to H_2O (mol H_2O m^{-2} s^{-1}), and photosynthetic rate (μmol CO_2 m^{-2} s^{-1}).

Leaf spectroscopy – We randomly selected five leaves within an hour of each branch being cut, and measured hemispherical reflectance near the mid-point between the main vein and the leaf edge (Asner & Martin, 2008). We used an ASD Fieldspec 4 with a fibre optic cable, contact

probe and a leaf clip (Analytical Spectral Devices, Boulder, Colorado, USA). The spectrometer records 2175 bands spanning the 325–2500 nm wavelength region. We corrected for small discontinuities between spectral bands (~950 and ~1750 nm), where the instrument transitions from one sensor to another. Measurements were collected with 136-ms integration time per spectrum (Asner & Martin, 2008; Doughty, Asner, et al., 2011). To ensure measurement quality, the spectrometer was calibrated for dark current and stray light, and white-referenced to a calibration panel (Spectralon, Labsphere, Durham, New Hampshire, USA) after each branch(Asner & Martin, 2008; Doughty, Field, et al., 2011). The spectrometer was optimized after every branch so the light levels did not saturate. For each measurement, 25 spectra were averaged together to increase the signal-to-noise ratio of the data.

Data analysis - We used the Partial Least Squares Regression (PLSR) modelling approach to predict leaf traits with spectral information (Geladi & Kowalski, 1986). PLSR incorporates all the spectral information within each leaf reflectance measurement, eventually reducing all spectral data (400-2500 nm) down to a relatively few, uncorrelated latent factors. This approach has been used successfully to predict plant traits across a wide range of ecosystems, including tropical forests (Asner & Martin, 2008; Serbin et al., 2014). We used the PLSregress command in Matlab (Matlab, MathWorks Inc., Natick, MA, USA) to establish predictive models for LMA, Asat, wood density (estimated with tree species and a lookup table (Chave et al., 2009)) and tree mortality (Doughty, Asner, et al., 2011). To avoid over-fitting the number of latent factors we minimized the mean square error with K-fold cross validation (set as an upper bound as 30). To avoid issues of pseudo replication, we emphasize that the unit of analysis in these analyses is the leaf. To create a completely independent testing dataset, we used the above method on 70% of

our data to calibrate our model and then the remaining 30% to test the accuracy of our model. We evaluated the accuracy of our modelled estimates using two main metrics: r^2 and root mean square error (RMSE)/mean. We graded our results as high precision and accuracy ($r^2 > 0.70$; %RMSE < 15%), medium precision and accuracy ($r^2 > 0.50$%; % RMSE < 30%), low precision and accuracy ($r^2 > 0.50$; % RMSE > 30%). We also calculated NDVI for our five study periods as NDVI = (NIR-red)/(NIR+red) where we use 1000 nm for NIR and 650 nm for red.

Statistical tests – For our leaf spectral measurements, for each 1 nm bandwidth, we determined statistical significance ($P<0.05$) between trees within 50 days of mortality and prior to this with a paired t-test (Matlab, Mathworks). To understand significant differences between % water, LMA, R_{dark}, and A_{sat}, we used a t-test. To understand the impact of the girdling between % water, LMA, R_{dark}, and A_{sat} over time, we used a repeated measures ANOVA.

262

263 **Results**

264 The field campaigns overlapped with the 2016 El Niño in Borneo (Figure 1b).
265 Campaign 1 (C1- Jan-21) took place before the period of peak drought and temperature, C3
266 (March -16) was conducted during the peak of the drought and high temperatures, and by C5
267 (June-16) the rains had returned. After C1, all the trees in the girdled plot had their phloem
268 tissue removed in a 10 cm band. Given the downward flux of sugars from the canopy, we might
269 expect an initial build-up of sugars above the girdle followed by eventual tree death as carbon
270 starvation below the girdle impacted tree function, particularly in the roots. Companion papers
271 explore the causes of tree death and the impacts on plant hydraulics and soil respiration.
272 There was little change in leaf reflectance (400-2500 nm) between C1 and C2 (Figure 2)
273 in both the drought and girdled plots. We expected few spectral changes during this short
274 interval between C1 and C2 (Jan-21 to Feb-10) for the natural drought plots, but we were
275 surprised there were also few changes for the girdled plots since these trees experienced a
276 significant trauma. In the later campaigns (C3 to C5 01-Mar to 08-Jun), there were large (~0.03
277 reflectance units) increases in NIR reflectance (750-1500 nm) in both the girdled and natural
278 drought plots (Figure 2 a and b). Reflectance in the visible wavelengths was lower during peak
279 drought (C3) compared to when the rains returned (C4 and C5). The girdled plots showed a
280 consistent increase in visible reflectance. Spectral reflectance increased in the SWIR bands over
281 time during the drought and there were few changes in the girdled plot except for the final
282 campaign where there was a decrease. Figure 2 displays all spectral data taken during each
283 campaign and therefore, changes in spectral properties in the girdled plot might also have
284 resulted from species changes because certain tree species died sooner than others, changing the

285 species composition as the experiment continued. To address this, in figure 5, we compare
286 spectroscopy for only trees that died.

287 Our average A_{sat} values across the campaigns for the girdled plot (3.7 μmol CO_2 m^{-2} s^{-1})
288 and the drought plot (4.7 μmol CO_2 m^{-2} s^{-1}) were slightly lower, but within 95% confidence
289 intervals of values from a nearby campaign in Borneo (old growth plots - 4.1 μmol CO_2 m^{-2} s^{-1}
290 (2.7–5.5 = 95% confidence interval) and selectively logged plots - 7.0 μmol CO_2 m^{-2} s^{-1} (5.7–
291 8.4)) (Both et al., 2019). Our average R_{dark} values across the campaigns for the girdled plot (-0.82
292 μmol CO_2 m^{-2} s^{-1}) and the drought plot (-0.83 μmol CO_2 m^{-2} s^{-1}) were likewise slightly less
293 negative than the values from Both et al 2019 of –1.0 μmol CO_2 m^{-2} s^{-1} (–0.9 to –1.2) for the old
294 growth plots and –1.3 μmol CO_2 m^{-2} s^{-1} (–1.1 to –1.4) for the selectively logged plots. Light
295 saturated leaf photosynthesis and R_{dark} varied between the wet and dry seasons in both plots over
296 the measurement period (Figure 3). Following the return of the rains, A_{sat} increased in both the
297 drought and girdled plots in C5. Surprisingly, the surviving girdled trees had the highest
298 photosynthetic rates of all the campaigns in C5 despite the damaged phloem. Dark respiration
299 was at its lowest in C3 and 4 during the peak of the drought. In both groups, changes in R_{dark}
300 mirrored those of A_{sat}. The ratio R_{dark}/ A_{sat} also varied between the wet and dry seasons, with the
301 exception of C4, where the drought plot was less efficient with greater carbon loss per carbon
302 gain. Leaf water content (% leaf water) was also at its lowest in C3 and 4 during the peak of the
303 drought but recovered by C5 (Figure 3e), but we did not find significant effects over time. NDVI
304 was lowest in C3 for both the girdle and drought plots but increased in C4 and C5 (Figure 3f). A
305 repeated measures ANOVA showed no significant differences between A_{sat}, R_d, and LMA over
306 time between the girdled and drought plots across the four campaigns (C1 was prior to the girdle)
307 suggesting the girdling had little overall impact of on leaf physiology.

To understand how the drought and girdling impacted leaf spectral properties in different ways and how these link to functional traits, we binned our results into groups of trees with either high (>0.5 g cm^3 N= 359 leaves/Campaign) or low wood density (<0.5 g cm^3 N= 830 leaves/Campaign) (Figure 4). During the drought, tree species with lower density showed an increase in leaf reflectance compared to species with higher density wood. For example, during the drought, tree species with lower wood density increased leaf reflectance by ~0.05 in the NIR and ~0.01 SWIR more than tree species with higher density wood, with fewer significant changes ($P<0.05$) in the visible bands. In contrast, the high wood density tree species show a stronger reaction to the girdling than the low wood density species, again with large increases in reflectance in the NIR and SWIR bands.

We then compared near death leaf reflectance (within 50 days of dying) to leaf reflectance from the same trees, during an earlier period, not near to death (Figure 5). By C5, 38 trees or 18% percent of all girdled trees had died. There were large (0.03-0.05 reflectance units) and significant decreases ($P<0.05$) in leaf reflectance in the visible bands and the red edge as tree death approached. Close to mortality, there were also large (0.02) and significant increases ($P<0.05$) in leaf reflectance in NIR and SWIR bands. Next, we investigated how drought conditions, caused by the ENSO event, affected leaf spectral properties in trees which died naturally in the non-girdled control plot. In the control plot, only one tree died from drought that was intensively sampled for functional traits. We observed similar significant changes along the same pre-death timeline, in leaf reflectance in this tree as observed in the trees that died following the girdling treatment: reductions in reflectance occurred in the red, the NIR and SWIR bands. However, there was a significant peak in the red edge in the opposite direction

compared to the girdling study. The wavelengths that show similarities for both types of death were: red (650-700nm), the NIR (1000 -1400nm) and SWIR bands (2000-2400nm).

For both the girdled and non-girdled trees, there were highly significant changes ($P<0.0001$) to the potential carbon balance (R_{dark} /A_{sat} – Figure 6e and f) of the leaves just prior to death (i.e. within 50 days). In both the drought and the girdled plots, there were significant increases in R_{dark} and significant decreases in A_{sat} (Figure 6). This combination of increased respiration and decreased photosynthesis should reduce the carbon available to the tree (again dependent on stomatal conductance changes). There was no significant change in LMA among the girdled trees. In contrast, in the tree that died from drought in the non-girdled plot, the leaves had significantly higher LMA and lower % water near to death. We do not know if this was a result of a changing cohort of leaves present on the sampled branch (i.e. leaves with lower LMA senesced sooner) or if all leaves changed their LMA via altered density prior to death (less likely as structural carbon is fixed).

Finally, we used PLSR to predict changes in physiology and time to death with spectroscopy (Figure 7). We used the primary weighting (right side of figure 7) to understand which spectral regions are most important (deviations from 0). Spectroscopy predicted % water and LMA well with an r^2 of 0.72 and 0.74 respectively and RMSE/mean of 0.07 and 0.14 (similar to many other studies with high precision and high accuracy (Asner and Martin 2008, Doughty et al 2011) (RMSE = 0.04 and 14.5, RMSE/std = 0.57 and 0.61, # of PLS weights = 30)). The primary weighting is in the NIR and SWIR bands which is typical of traits relating to structure. Spectroscopy predicted maximum photosynthetic rate (A_{sat}) with an r^2 of 0.66 and RMSE/mean of 0.69 (medium precision but low accuracy) (RMSE = 3.3, RMSE/std = 0.74, # of PLS weights = 25/30) and wood density with an r^2 of 0.41 and RMSE/mean of 0.24 (low

353 precision but medium accuracy) (RMSE = 0.12, RMSE/std = 0.94, # of PLS weights = 15). The
354 primary weighting of A_{sat} was in the visible bands (likely related to chlorophyll content) and for
355 wood density in NIR and SWIR >1000 nm (likely related to variations in LMA and leaf
356 structure). Finally, we predicted time to death with spectroscopy and the PLSR technique with an
357 r^2 of 0.68 and RMSE/mean of 0.55 (medium precision and low accuracy) (RMSE = 82,
358 RMSE/std = 0.81, # of PLS weights = 30). The primary weighting shows similarity with Figure
359 5 with important spectral regions in the visible (related to photosynthetic characteristics), the
360 NIR (related to structure) and SWIR bands (related to water bands).

361

362

Discussion

Leaf spectroscopy - Identification of tropical trees susceptible to mortality through hyperspectral imagery could provide a powerful tool in examining recently reported increases in tree mortality rates across the tropics(Brienen et al., 2015; Hubau et al., 2020). By contributing to "environmental surveillance," the use of hyperspectral data would have a wide range of applications from the prediction of tree death from heat stress, pests, pathogens or illegal logging. Moreover, this technique could enable us to identify potential tipping points in tropical forests, with wider ramifications for the development of adaptive forest management strategies in the future.

Based on these results, future mortality is potentially predictable using hyperspectral data for up to 50 days in advance of tree death (Figure 7). We also observed a tree that died naturally from drought, and saw that there were regions of spectral overlap with the signal from trees killed by girdling in terms of the wavelengths that changed prior to tree death; e.g. red (650-700nm), the NIR (1000 -1400nm) and SWIR bands (2000-2400nm) (blue circles in Figure 5), but it is difficult to draw conclusions from just one tree. Another venue of remotely sensing stress would be through predicting changes in leaf water content which declined in leaves during the drought (drought and gridled trees) and <50 days prior to death (only the drought tree) (Figures 3 and 6), and is highly predictable, with high precision and accuracy (Figure 7). This gives us some confidence that the spectral changes may be general to mortality and not specific to girdling-induced mortality. We demonstrate only changes in leaf reflectance and not overall canopy reflectance. It is important to differentiate between leaf versus canopy reflectance (as seen from aircraft or space) because the latter also incorporates forest structural changes (such as variations in LAI, branch architecture, stem density), which were not measured. Leaf spectral

properties strongly influence canopy spectral properties especially in certain wavelengths (Asner and Martin 2008), but changes in other properties, like LAI, would complicate the signal. Leaf-level analyses may also suffer from survivorship bias where the leaves that fare the worst under drought drop first. Large shifts in the spectral regions shown in Fig 5 may be indicative of tree mortality and should be tested with hyperspectral aircraft data in the region for confirmation (Swinfield et al., 2019). A previous study using Hyperion hyperspectral satellite data over an Amazonian drought experiment showed similar declines in magnitude in the NIR and VIS regions as our study (Fig 5) (Asner et al., 2004).

Surprisingly, leaf spectral properties did not vary greatly during the period immediately following tree girdling (~1 week). Previous studies have quantified changes in non-photosynthetic vegetation to estimate regional selective logging impacts (Asner et al., 2005). Here we show that significant trauma to the trunk (i.e. the girdling treatment) did not immediately result in changes to leaf spectral properties, but that leaf spectral properties did change significantly within 50 days of tree death. We hypothesize that > 7 days is the time needed to change the biochemistry, physiology and metabolism of leaves to respond to substantive environmental stress because we saw little change between C1 and C2. This indicates that >7 days but <50 are necessary for leaf spectral changes to occur (Figure 5), which could constrain timing for a potential new technique to identify damage to trees from selective logging.

Do we succeed in predicting mortality because there are changes in short-term physiological status (e.g. reduced relative % water content in leaves) or because certain trees are just more likely to die than others due to their constitutive traits (e.g. lower LMA linked to a different life history strategy)? In the girdled study, LMA and % water did not change

409 significantly prior to death, but leaf gas exchange metrics did (A_{sat} and R_{dark}), shown in the large
410 and significant changes in the visible and red edge bands (Fig 5). However, the drought-
411 associated tree death event was accompanied by a significant change in LMA and % water
412 content, and the spectral analysis showed a further correlation with significant changes in the
413 NIR and water bands (Fig 5). Therefore, it seems a combination of changes in leaf structure,
414 physiological status and associated reflectance traits combine to enable mortality to be
415 predictable.

416 It should be noted that prior to this study our plots had been extensively logged (i.e. four
417 times since the 1970's,), with 46 to 54 Mg C ha^{-1} cumulative extracted biomass in the area
418 (Riutta et al., 2018). Logging has been shown with hyperspectral imagery in Borneo to lower
419 canopy foliar nutrient concentrations and to decrease nutrient availability (Swinfield et al.,
420 2019). Our results are therefore biased towards logged/low foliar nutrient forests, although our
421 dataset does include late-successional species as well. However, most forests (72%) in the study
422 region have been selectively logged, and our results should be valid for these forests (Bryan et
423 al., 2013).

424 **Leaf physiology** - Leaf dark respiration, R_{dark}, was at its lowest during the peak of the drought,
425 in campaigns C3 and C4. This stands in contrast to some other tropical rainforest leaf respiration
426 studies during natural and artificial drought that have seen increases in leaf respiration rates
427 (Miranda et al., 2005; Rowland et al., 2015), although recent intensive survey results suggest that
428 the response to experimental drought was taxon-specific rather than observed across a wide
429 range of species (Rowland et al in review). Leaf R_{dark} also did not increase in the leaves of
430 girdled trees despite potential increases in leaf NSC content (as they could not be transported
431 towards the roots following the girdling). Other studies have shown a decrease in overall tree

respiration during drought periods as compared to before a drought (Doughty et al., 2015), and this is a similar pattern shown at our plots (Riutta et al 2020).

We also observed both increased R_{dark} and decreased A_{sat} 50 days prior to tree death (Fig 6), which in combination, are very likely to reduce the carbon available in leaf tissue (although net carbon balance is also dependent on changes in stomatal conductance and light availability). This decreased carbon balance, in turn, could increase the likelihood of carbon starvation (McDowell et al., 2018) and reduce the availability of carbon (or more accurately non-structural carbohydrates) for possible embolism repair in the water conducting xylem tissue (Sala et al., 2012). It is also interesting to note that the highest average photosynthetic capacity (A_{sat}) for the girdled experiment were observed when the rains returned. We speculate that might be due to a growth or sink driven response where, after the return of available water there was increased growth (e.g. leaf flushing, xylem regrowth) to replace senesced tissue. We hypothesize that the increased growth results in a higher carbon sink leading to a higher demand for NSC with a consequent increase in A_{sat}. Overall, this is strong evidence that photosynthesis remains robust to perturbations, and that growth may be maintained preceding a mortality event as the plant attempts to recover damaged xylem capacity (Rowland et al., 2015; Meir et al., 2018).

Conclusion

Our key finding is that remote sensing using spectral imagery shows potential to identify trees at imminent risk of death (approximately 50 days prior) with significant ($P<0.05$) leaf spectral changes in the red (650-700 nm), the NIR (1000 -1400 nm) and SWIR bands (2000-2400 nm). This technique has widespread relevance and applicability for ecological/management surveillance, prediction of future vegetation and forest carbon dynamics. We suggest aircraft campaigns search for a large shift in visible, red edge, and NIR reflectance

and compare this to later observed tree mortality or possibly use past data to "hindcast" this technique for validity. For instance, we hypothesize that comparing hyperspectral aircraft flights before and after the 2016 drought might show large shifts in reflectance properties prior to tree mortality(Davies et al., 2019; Swinfield et al., 2019). This could also be of use for hyperspectral satellites like DESIS to predict changes in long term carbon fluxes associated with tree mortality (Krutz et al., 2019). The large significant changes in leaf reflectance observed here that were shared by both girdling- and drought-killed trees at the same timescale prior to mortality indicate that there could be a spectral indication of tropical tree mortality that has regional or wider application.

Tables

Table 1 – Tree species measured intensively in the drought and girdled plot aligned to show which species were measured in both plots.

Girdled Plot	Drought Plot
Adinandra borneensis,	*Adinandra borneensis,*
Brownlowia peltata,	
	Cariumna odontophyllum,
	Diplodiscus paniculatus,
	Dipterocarpus caudiferus,
Dryobalanops lanceolate,	*Dryobalanops lanceolate,*
Duabanga moluccana,	*Duabanga moluccana,*
	Endospermum peltatum,
Hydnocarpus anomalus,	
Leea aculeate,	
Lithocarpus blumeanus,	*Lithocarpus blumeanus,*
Litsea garciae,	
Lophopetalum sp.,	
Macaranga hypoleuca,	
Macaranga pearsonii,	*Macaranga pearsonii,*
	Mallotus leucodermis,
	Nauclea officinalis,
Neolamarckia cadamba,	*Neolamarckia cadamba,*
Nephelium rambutan,	
Parashorea malaanonan,	*Parashorea malaanonan,*
	Pleiocarpidia sandakanica,
	Pterospermum elongatum,
	Shorea gibbosa,
Shorea johorensis,	*Shorea johorensis,*
Shorea parvifolia.	
	Syzygium sp.,
	Trema orientalis

Figures

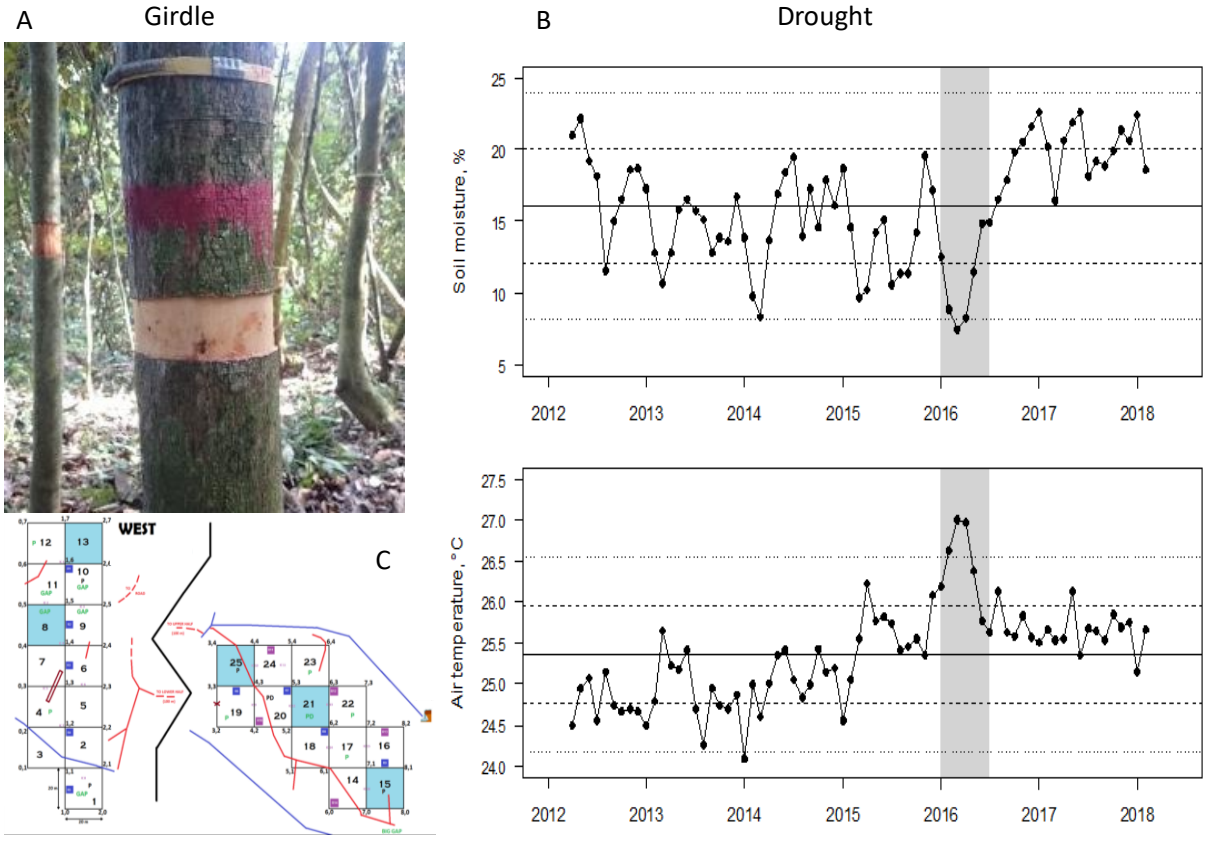

Figure 1. (A) An example tree that was girdled by stripping 10 cm of phloem in a ring around the tree. (B) Monthly volumetric soil moisture content at 20 cm depth (top) and air temperature (bottom) records at the study site. The horizontal continuous line denotes the long-term mean and the dashed lines denote 1 and 2 standard deviations. The grey region is the period of our measurements. (C) A schematic of the plot layout with the non-girdled trees in the section labelled West (the other section was girdled). The total area of the plot is 1 ha, with the two sections separated by approximately 200 m. The middle black line represents the river. Each individual square represents a 20 m ×20 m subplot. Red lines are trails and blue lines are small temporary streams.

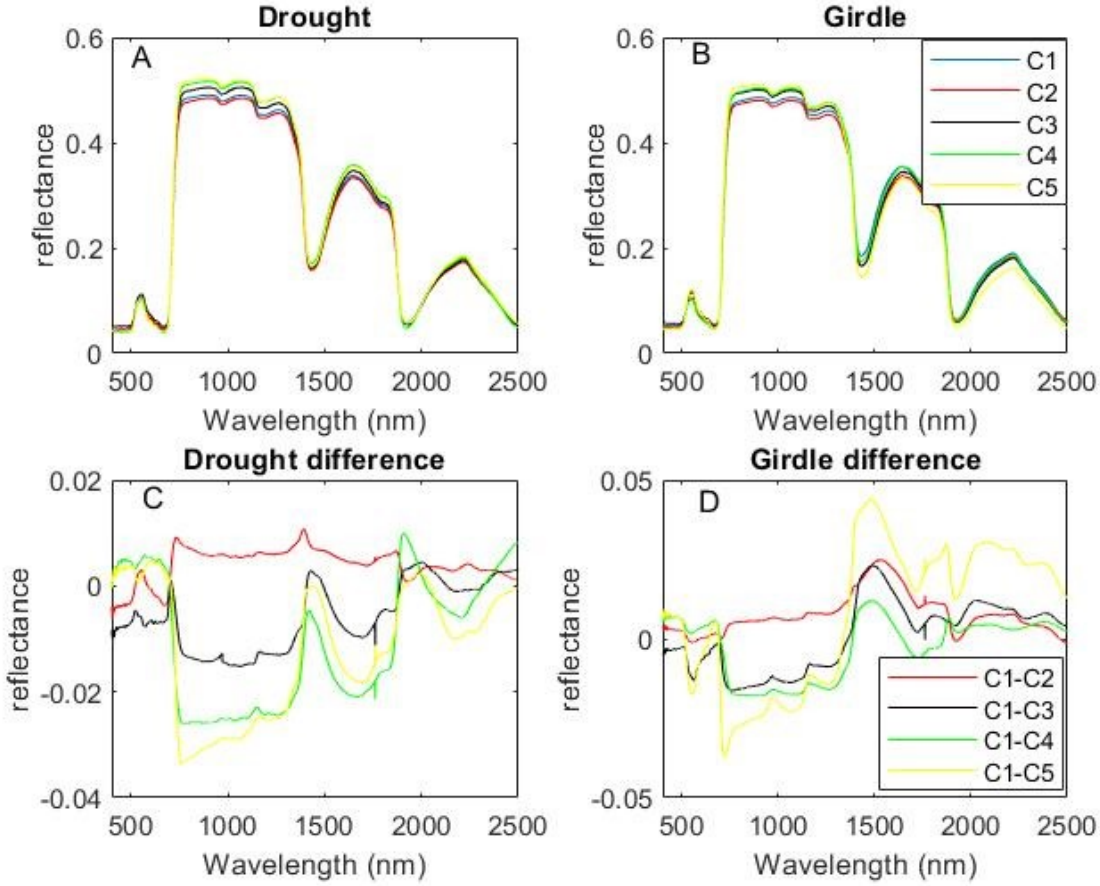

483

484 **Figure 2.** Leaf spectral properties (400-2500nm) for the drought (A) and girdled (B) plots for the 5
485 campaigns (Jan-June 2015). (bottom) The difference (C1-CX, where X=2-5) in leaf spectral properties
486 for the drought (C) and the girdled (D) plots. In each campaign, we sampled the same trees unless the
487 trees died. Reflectance factor is reflected incident light between 0-1.

488

489

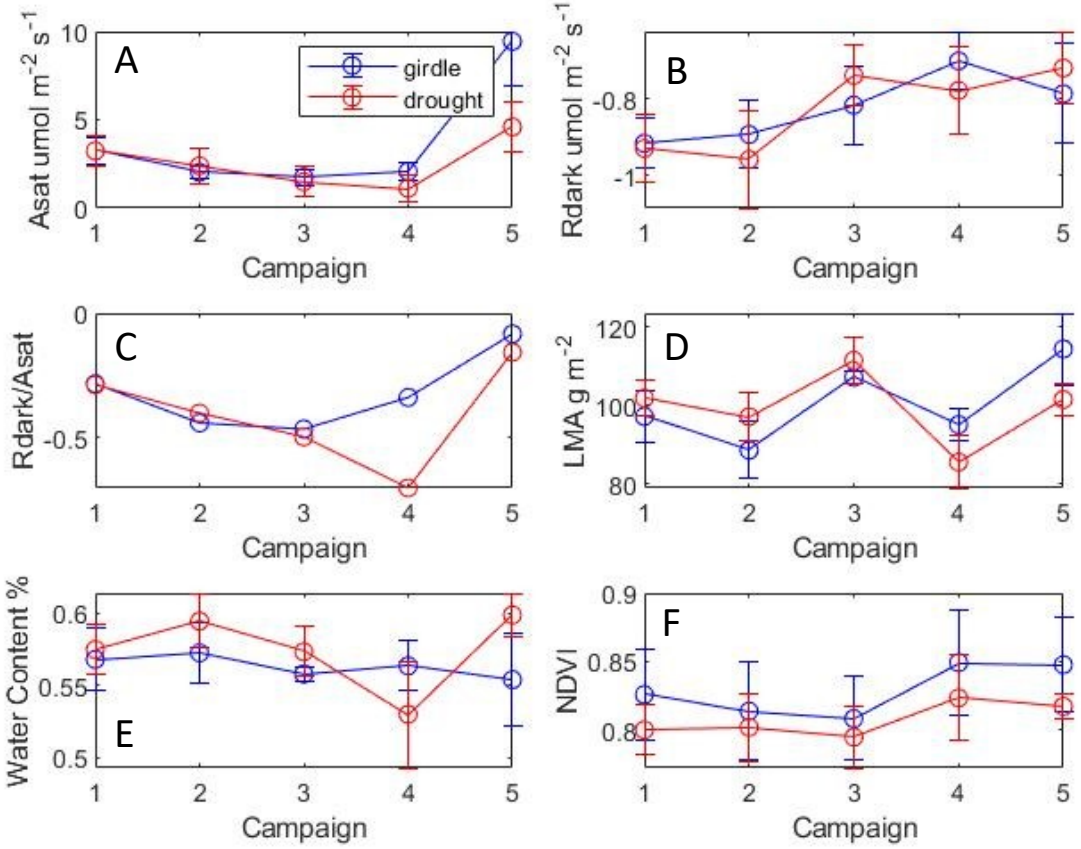

Figure 3. Average ± se (A_{sat}) photosynthetic capacity (A), (R_{dark}) leaf dark respiration (B), A_{sat} / R_{dark} (C) (LMA) leaf mass area (D), % leaf water (E) and NDVI (F) for the 5 campaigns for the control site (red) and the girdled site (blue). A_{sat} and R_d were collected at a standard temperature (30 °C) during all campaigns. We subtracted the initial difference (2 µmol m^{-2} sec^{-1}) in the top panel between the average C1 values to better highlight the impact of the girdling. Peak drought was C3 and the rains returned in C5.

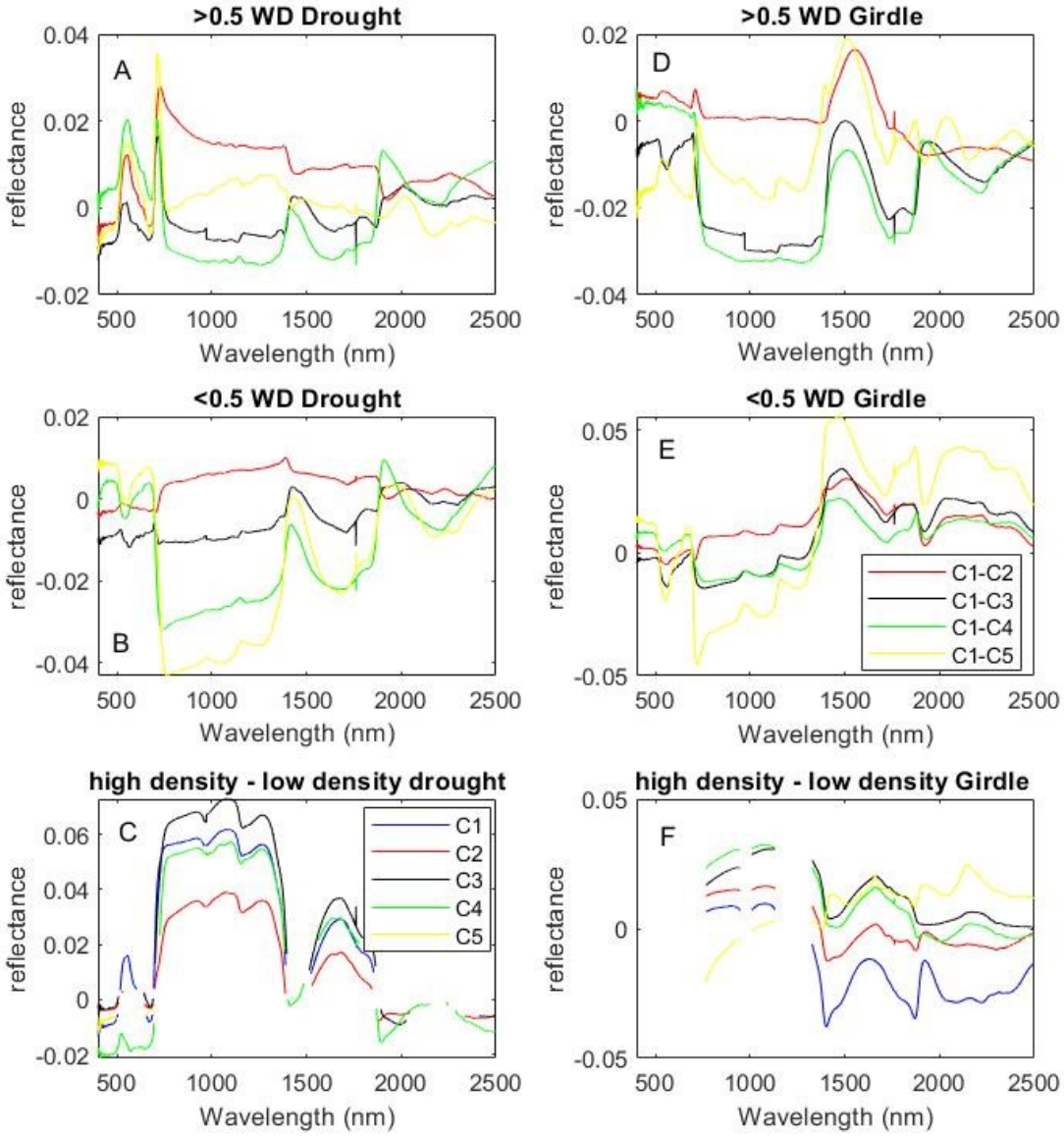

499

500 **Figure 4.** The change in leaf spectral properties (400-2500 nm) between campaigns comparing drought
501 plots for species with high wood density (density>0.5 g cm^{-3} - A), low wood density (density <0.5 g cm^{-3},
502 B), and the difference (C) through the 5 campaigns. The girdled plots for species with high wood density
503 (density>0.5 g cm^{-3} - D), low wood density (density <0.5 g cm^{-3}, E), and the difference (F). For the
504 difference plots, only significant (P<0.05) spectral regions are shown.

505

506

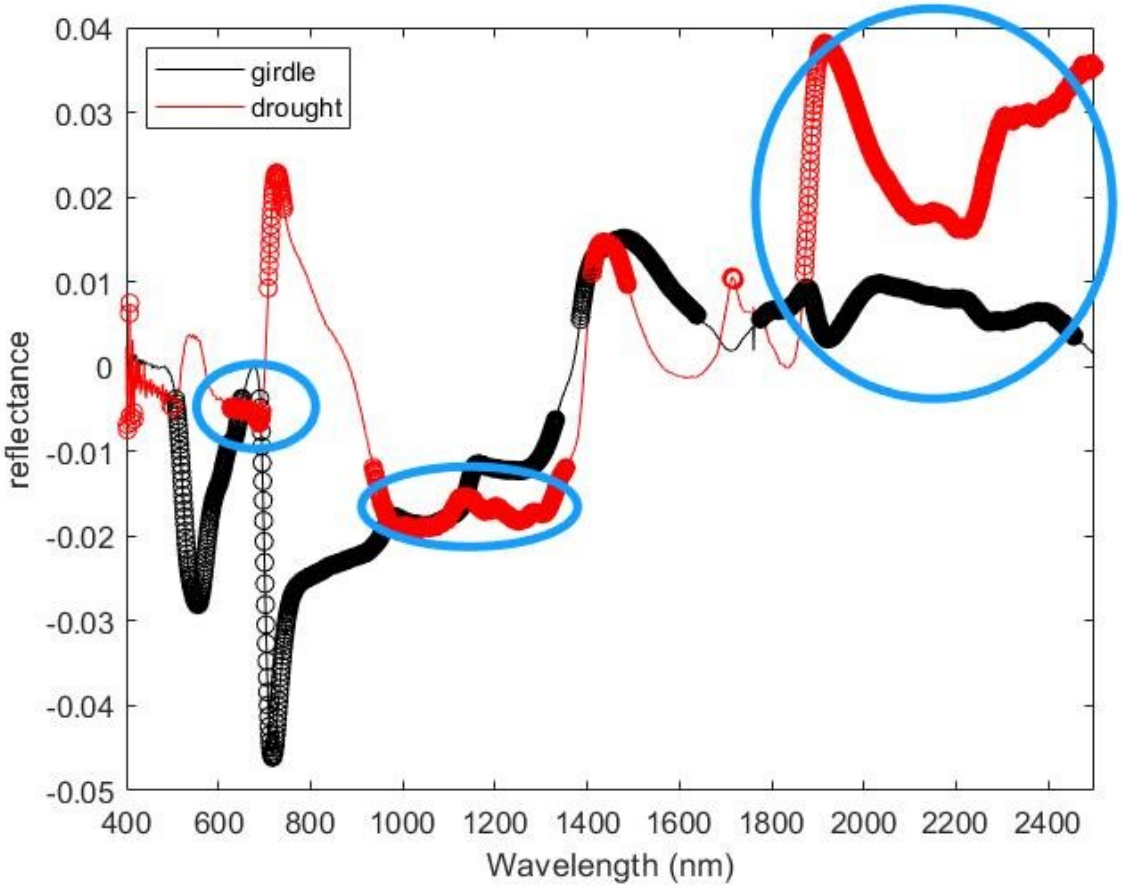

Figure 5 –The change (negative is a reduction in reflectance close to death) in leaf spectral properties from healthy leaves (>50 days from death) minus close to death leaves (<50 days from death) on a tree that died of natural drought (red, N=14 leaves) and trees that died during the girdling experiment (black, N=122 leaves). Dots show regions of significant change ($P<0.05$) using a paired t-test. Blue circled areas are key areas of spectral overlap.

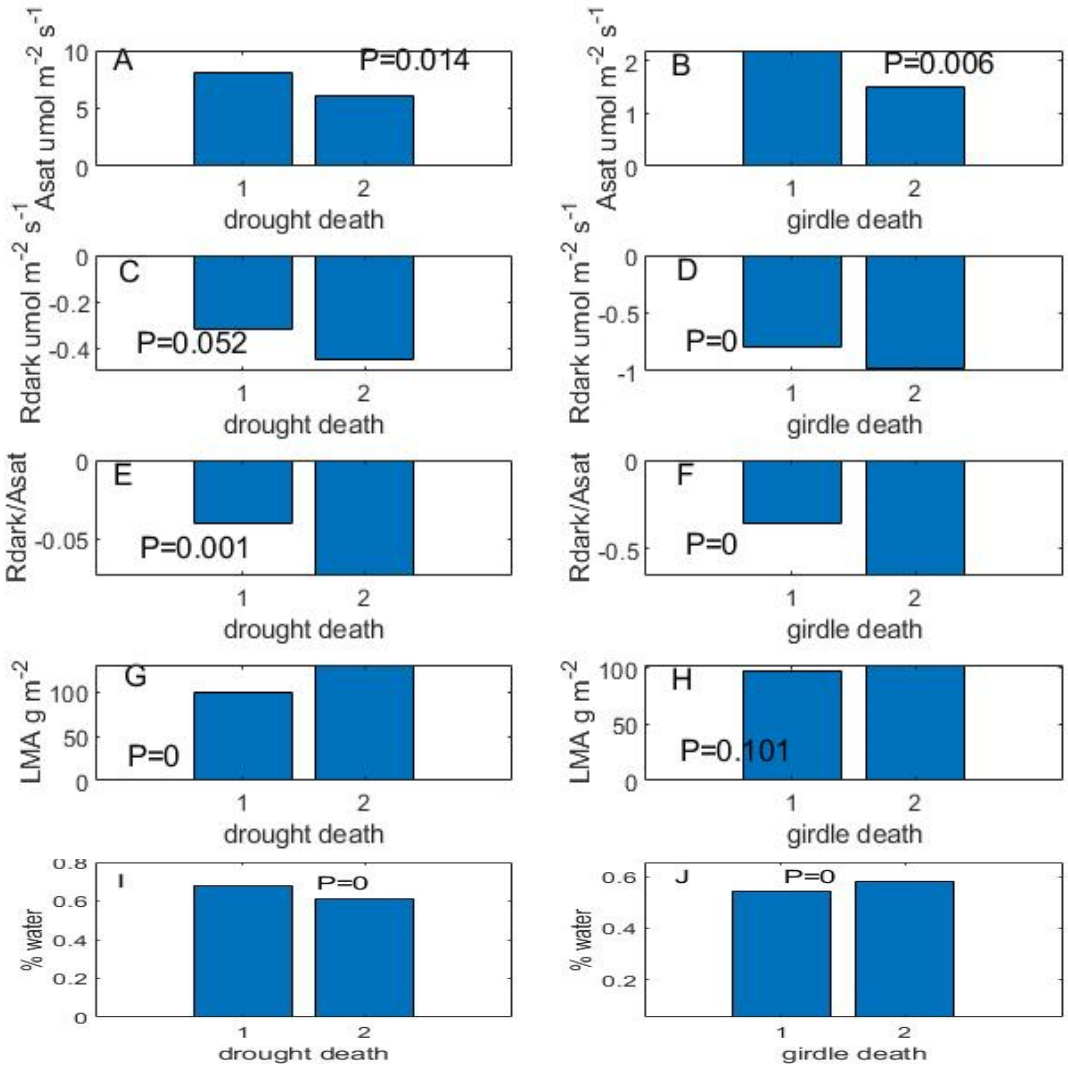

517

518 **Figure 6** – Comparison of the intensively monitored tree that died during the drought (left) and
519 the girdling experiment (right) for A_{sat} (A,B), R_{dark} (C,D), R_{dark}/ A_{sat} (E, F), LMA (G, H) and %
520 water (I, J) between initial values and values within 50 days of death. The P value listed is the
521 level of significance to three digits for a student's t-test. P=0 is a P value less than 0.0001.

522

523

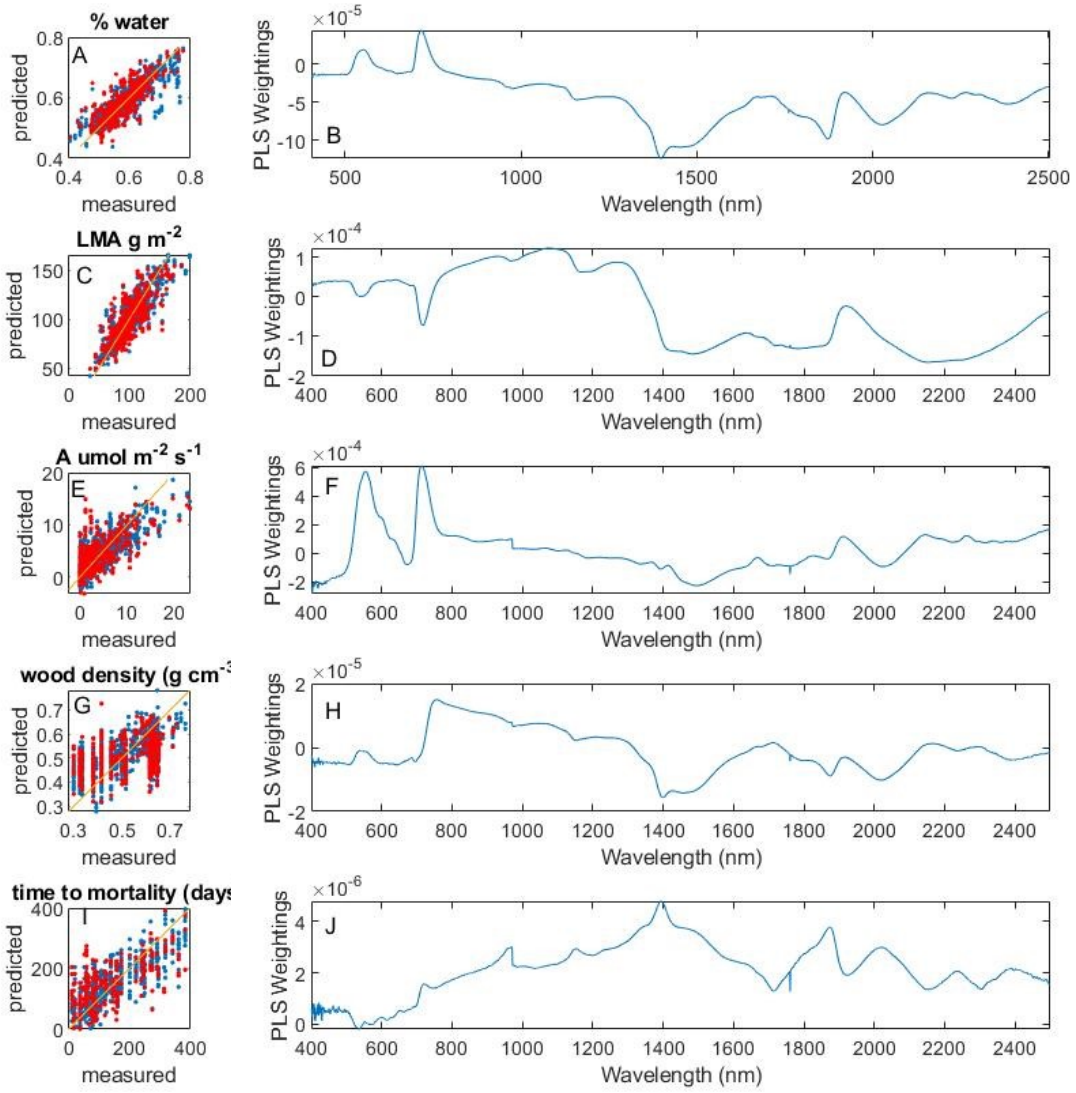

524

525 **Figure 7.** On the left is predictive power (measured vs predicted) for the PLSR analysis with the r^2 and
526 RMSE/mean calculated from the full dataset for various traits including % water (A, r^2=0.72, RMSE =
527 0.07), LMA (C, r^2=0.74, RMSE/mean = 0.14), Asat (E, r^2=0.66, RMSE/mean = 0.69), wood density (G,
528 r^2=0.41, RMSE/mean = 0.24), and time to tree death (I, r^2=0.68, RMSE/mean = 0.55). Red dots are the
529 data to train the model (70%) and the blue dots are the independent dataset (30%). Sample sizes to train
530 the models are as follows: % water – N=1035, LMA-N=1028, Asat- N=846, wood density – N= 841, tree
531 death – N=543. On the right is the primary weighting, which is the PLS weight that explains the most
532 variance in the data, multiplied by variance explained for % water (B), LMA (D), Asat (F), wood density
533 (H), and time to tree death (J).

534

Acknowledgements – We would like to acknowledge Dr. Rob Ewers for his role in setting up the SAFE experiment, Elelia Nahun, Dg Ku Shamirah binti Pg Bakar for their contributions to the field campaign, Unding Jami, Ryan Gray, Rostin Jantan, Suhaini Patik and Rohid Kailoh and the BALI and Lombok project research assistants.

Data Availability statement – The data and code that support the findings of this study are openly available in Data Dryad at http://doi.org/doi:10.5061/dryad.d51c5b01n.

References

Adams, H. D., Zeppel, M. J. B., Anderegg, W. R. L., Hartmann, H., Landhäusser, S. M., Tissue, D. T., et al. (2017). A multi-species synthesis of physiological mechanisms in drought-induced tree mortality. *Nature Ecology and Evolution*. https://doi.org/10.1038/s41559-017-0248-x

Anderegg, W. R. L., Klein, T., Bartlett, M., Sack, L., Pellegrini, A. F. A., Choat, B., & Jansen, S. (2016). Meta-analysis reveals that hydraulic traits explain cross-species patterns of drought-induced tree mortality across the globe. *Proceedings of the National Academy of Sciences of the United States of America*. https://doi.org/10.1073/pnas.1525678113

Anderegg, W. R. L., Konings, A. G., Trugman, A. T., Yu, K., Bowling, D. R., Gabbitas, R., et al. (2018). Hydraulic diversity of forests regulates ecosystem resilience during drought. *Nature*. https://doi.org/10.1038/s41586-018-0539-7

Asner, G. P., & Martin, R. E. (2008). Spectral and chemical analysis of tropical forests: Scaling from leaf to canopy levels. *Remote Sensing of Environment*. https://doi.org/10.1016/j.rse.2008.07.003

Asner, G. P., Nepstad, D., Cardinot, G., & Ray, D. (2004). Drought stress and carbon uptake in an Amazon forest measured with spaceborne imaging spectroscopy. *Proceedings of the National Academy of Sciences of the United States of America*, *101*(16), 6039 LP – 6044. https://doi.org/10.1073/pnas.0400168101

Asner, G. P., Knapp, D. E., Broadbent, E. N., Oliveira, P. J. C., Keller, M., & Silva, J. N. (2005). Ecology: Selective logging in the Brazilian Amazon. *Science*. https://doi.org/10.1126/science.1118051

Asner, G. P., Knapp, D. E., Anderson, C. B., Martin, R. E., & Vaughn, N. (2016). Large-scale climatic and geophysical controls on the leaf economics spectrum. *Proceedings of the National Academy of Sciences of the United States of America*. https://doi.org/10.1073/pnas.1604863113

Bartlett, M. K., Scoffoni, C., & Sack, L. (2012). The determinants of leaf turgor loss point and prediction of drought tolerance of species and biomes: A global meta-analysis. *Ecology Letters*. https://doi.org/10.1111/j.1461-0248.2012.01751.x

Bittencourt, P. R. L., Oliveira, R. S., da Costa, A. C. L., Giles, A. L., Coughlin, I., Costa, P. B., et al. (2020). Amazonian trees have limited capacity to acclimate plant hydraulic properties in response to long-term drought. *Global Change Biology*. https://doi.org/10.1111/gcb.15040

Both, S., Riutta, T., Paine, C. E. T., Elias, D. M. O., Cruz, R. S., Jain, A., et al. (2019). Logging and soil nutrients independently explain plant trait expression in tropical forests. *New Phytologist*. https://doi.org/10.1111/nph.15444

Brienen, R. J. W., Phillips, O. L., Feldpausch, T. R., Gloor, E., Baker, T. R., Lloyd, J., et al. (2015). Long-term decline of the Amazon carbon sink. *Nature*.

https://doi.org/10.1038/nature14283

Bryan, J. E., Shearman, P. L., Asner, G. P., Knapp, D. E., Aoro, G., & Lokes, B. (2013). Extreme Differences in Forest Degradation in Borneo: Comparing Practices in Sarawak, Sabah, and Brunei. *PLoS ONE*. https://doi.org/10.1371/journal.pone.0069679

Chave, J., Coomes, D., Jansen, S., Lewis, S. L., Swenson, N. G., & Zanne, A. E. (2009). Towards a worldwide wood economics spectrum. *Ecology Letters*. https://doi.org/10.1111/j.1461-0248.2009.01285.x

Clark, D. A. (2004). Sources or sinks? The responses of tropical forests to current and future climate and atmospheric composition. In *Philosophical Transactions of the Royal Society B: Biological Sciences*. https://doi.org/10.1098/rstb.2003.1426

da Costa, A. C. L., Galbraith, D., Almeida, S., Portela, B. T. T., da Costa, M., de Athaydes Silva Junior, J., et al. (2010). Effect of 7 yr of experimental drought on vegetation dynamics and biomass storage of an eastern Amazonian rainforest. *New Phytologist*. https://doi.org/10.1111/j.1469-8137.2010.03309.x

Curran, P. J. (1989). Remote sensing of foliar chemistry. *Remote Sensing of Environment*. https://doi.org/10.1016/0034-4257(89)90069-2

Davies, A. B., Oram, F., Ancrenaz, M., & Asner, G. P. (2019). Combining behavioural and LiDAR data to reveal relationships between canopy structure and orangutan nest site selection in disturbed forests. *Biological Conservation*. https://doi.org/10.1016/j.biocon.2019.01.032

Díaz, S., Kattge, J., Cornelissen, J. H. C., Wright, I. J., Lavorel, S., Dray, S., et al. (2016). The global spectrum of plant form and function. *Nature*. https://doi.org/10.1038/nature16489

Doughty, C. E., & Goulden, M. L. (2009a). Are tropical forests near a high temperature threshold? *Journal of Geophysical Research: Biogeosciences*. https://doi.org/10.1029/2007JG000632

Doughty, C. E., & Goulden, M. L. (2009b). Seasonal patterns of tropical forest leaf area index and CO2 exchange. *Journal of Geophysical Research: Biogeosciences*. https://doi.org/10.1029/2007JG000590

Doughty, C. E., Field, C. B., & McMillan, A. M. S. (2011). Can crop albedo be increased through the modification of leaf trichomes, and could this cool regional climate? *Climatic Change*. https://doi.org/10.1007/s10584-010-9936-0

Doughty, C. E., Asner, G. P., & Martin, R. E. (2011). Predicting tropical plant physiology from leaf and canopy spectroscopy. *Oecologia*. https://doi.org/10.1007/s00442-010-1800-4

Doughty, C. E., Metcalfe, D. B., Girardin, C. A. J., Amézquita, F. F., Cabrera, D. G., Huasco, W. H., et al. (2015). Drought impact on forest carbon dynamics and fluxes in Amazonia. *Nature*. https://doi.org/10.1038/nature14213

Doughty, C. E., Santos-Andrade, P. E., Goldsmith, G. R., Blonder, B., Shenkin, A., Bentley, L. P., et al. (2017). Can Leaf Spectroscopy Predict Leaf and Forest Traits Along a Peruvian Tropical Forest Elevation Gradient? *Journal of Geophysical Research: Biogeosciences*.

https://doi.org/10.1002/2017JG003883

Ewers, R. M., Didham, R. K., Fahrig, L., Ferraz, G., Hector, A., Holt, R. D., et al. (2011). A large-scale forest fragmentation experiment: The stability of altered forest ecosystems project. *Philosophical Transactions of the Royal Society B: Biological Sciences*. https://doi.org/10.1098/rstb.2011.0049

Fyllas, N. M., Quesada, C. A., & Lloyd, J. (2012). Deriving Plant Functional Types for Amazonian forests for use in vegetation dynamics models. *Perspectives in Plant Ecology, Evolution and Systematics*. https://doi.org/10.1016/j.ppees.2011.11.001

Geladi, P., & Kowalski, B. R. (1986). Partial least-squares regression: a tutorial. *Analytica Chimica Acta*. https://doi.org/10.1016/0003-2670(86)80028-9

Gvozdevaite, A., Oliveras, I., Domingues, T. F., Peprah, T., Boakye, M., Afriyie, L., et al. (2018). Leaf-level photosynthetic capacity dynamics in relation to soil and foliar nutrients along forest–savanna boundaries in Ghana and Brazil. *Tree Physiology*. https://doi.org/10.1093/treephys/tpy117

Hubau, W., Lewis, S. L., Phillips, O. L., Affum-Baffoe, K., Beeckman, H., Cuní-Sanchez, A., et al. (2020). Asynchronous carbon sink saturation in African and Amazonian tropical forests. *Nature*. https://doi.org/10.1038/s41586-020-2035-0

Jacquemoud, S., Verhoef, W., Baret, F., Bacour, C., Zarco-Tejada, P. J., Asner, G. P., et al. (2009). PROSPECT + SAIL models: A review of use for vegetation characterization. *Remote Sensing of Environment*. https://doi.org/10.1016/j.rse.2008.01.026

Krutz, D., Müller, R., Knodt, U., Günther, B., Walter, I., Sebastian, I., et al. (2019). The Instrument Design of the DLR Earth Sensing Imaging Spectrometer (DESIS). *Sensors* . https://doi.org/10.3390/s19071622

Malhi, Y., Gardner, T. A., Goldsmith, G. R., Silman, M. R., & Zelazowski, P. (2014). Tropical Forests in the Anthropocene. *Annual Review of Environment and Resources*. https://doi.org/10.1146/annurev-environ-030713-155141

Maréchaux, I., Bartlett, M. K., Sack, L., Baraloto, C., Engel, J., Joetzjer, E., & Chave, J. (2015). Drought tolerance as predicted by leaf water potential at turgor loss point varies strongly across species within an Amazonian forest. *Functional Ecology*. https://doi.org/10.1111/1365-2435.12452

McDowell, N., Allen, C. D., Anderson-Teixeira, K., Brando, P., Brienen, R., Chambers, J., et al. (2018). Drivers and mechanisms of tree mortality in moist tropical forests. *New Phytologist*. https://doi.org/10.1111/nph.15027

Meir, P., Wood, T. E., Galbraith, D. R., Brando, P. M., Da Costa, A. C. L., Rowland, L., & Ferreira, L. V. (2015). Threshold Responses to Soil Moisture Deficit by Trees and Soil in Tropical Rain Forests: Insights from Field Experiments. *BioScience*. https://doi.org/10.1093/biosci/biv107

Miranda, E. J., Vourlitis, G. L., Filho, N. P., Priante, P. C., Campelo, J. H., Suli, G. S., et al. (2005). Seasonal variation in the leaf gas exchange of tropical forest trees in the rain forest–savanna transition of the southern Amazon Basin. *Journal of Tropical Ecology*, *21*(4), 451–

460. https://doi.org/DOI: 10.1017/S0266467405002427

Morton, D. C., Nagol, J., Carabajal, C. C., Rosette, J., Palace, M., Cook, B. D., et al. (2014). Amazon forests maintain consistent canopy structure and greenness during the dry season. *Nature*. https://doi.org/10.1038/nature13006

Nepstad, D. C., Tohver, I. M., David, R., Moutinho, P., & Cardinot, G. (2007). Mortality of large trees and lianas following experimental drought in an amazon forest. *Ecology*. https://doi.org/10.1890/06-1046.1

Niinemets, Ü. (2001). Global-scale climatic controls of leaf dry mass per area, density, and thickness in trees and shrubs. *Ecology*. https://doi.org/10.1890/0012-9658(2001)082[0453:GSCCOL]2.0.CO;2

Nunes, M. H., Both, S., Bongalov, B., Brelsford, C., Khoury, S., Burslem, D. F. R. P., et al. (2019). Changes in leaf functional traits of rainforest canopy trees associated with an El Nino event in Borneo. *Environmental Research Letters*. https://doi.org/10.1088/1748-9326/ab2eae

Phillips, O. L., Aragão, L. E. O. C., Lewis, S. L., Fisher, J. B., Lloyd, J., López-González, G., et al. (2009). Drought sensitivity of the amazon rainforest. *Science*. https://doi.org/10.1126/science.1164033

Poorter, H., Niinemets, Ü., Poorter, L., Wright, I. J., & Villar, R. (2009). Causes and consequences of variation in leaf mass per area (LMA): A meta-analysis. *New Phytologist*. https://doi.org/10.1111/j.1469-8137.2009.02830.x

Poorter, L., Wright, S. J., Paz, H., Ackerly, D. D., Condit, R., Ibarra-Manríquez, G., et al. (2008). Are functional traits good predictors of demographic rates? Evidence from five neotropical forests. *Ecology*. https://doi.org/10.1890/07-0207.1

Rifai, S. W., Girardin, C. A. J., Berenguer, E., Del Aguila-Pasquel, J., Dahlsjö, C. A. L., Doughty, C. E., et al. (2018). ENSO Drives interannual variation of forest woody growth across the tropics. *Philosophical Transactions of the Royal Society B: Biological Sciences*. https://doi.org/10.1098/rstb.2017.0410

Rifai, S. W., Li, S., & Malhi, Y. (2019). Coupling of El Niño events and long-term warming leads to pervasive climate extremes in the terrestrial tropics. *Environmental Research Letters*. https://doi.org/10.1088/1748-9326/ab402f

Riutta, T., Malhi, Y., Kho, L. K., Marthews, T. R., Huaraca Huasco, W., Khoo, M., et al. (2018). Logging disturbance shifts net primary productivity and its allocation in Bornean tropical forests. *Global Change Biology*, *24*(7), 2913–2928. https://doi.org/10.1111/gcb.14068

Rowland, L., Da Costa, A. C. L., Galbraith, D. R., Oliveira, R. S., Binks, O. J., Oliveira, A. A. R., et al. (2015). Death from drought in tropical forests is triggered by hydraulics not carbon starvation. *Nature*. https://doi.org/10.1038/nature15539

Rowland, Lucy, Lobo-do-Vale, R. L., Christoffersen, B. O., Melém, E. A., Kruijt, B., Vasconcelos, S. S., et al. (2015). After more than a decade of soil moisture deficit, tropical rainforest trees maintain photosynthetic capacity, despite increased leaf respiration. *Global Change Biology*. https://doi.org/10.1111/gcb.13035

Rowland, Lucy, Zaragoza-Castells, J., Bloomfield, K. J., Turnbull, M. H., Bonal, D., Burban, B., et al. (2017). Scaling leaf respiration with nitrogen and phosphorus in tropical forests across two continents. *New Phytologist*. https://doi.org/10.1111/nph.13992

Sala, A., Woodruff, D. R., & Meinzer, F. C. (2012). Carbon dynamics in trees: Feast or famine? *Tree Physiology*. https://doi.org/10.1093/treephys/tpr143

Saleska, S. R., Didan, K., Huete, A. R., & Da Rocha, H. R. (2007). Amazon forests green-up during 2005 drought. *Science*. https://doi.org/10.1126/science.1146663

Samanta, A., Ganguly, S., Hashimoto, H., Devadiga, S., Vermote, E., Knyazikhin, Y., et al. (2010). Amazon forests did not green-up during the 2005 drought. *Geophysical Research Letters*. https://doi.org/10.1029/2009GL042154

Sapes, G., Roskilly, B., Dobrowski, S., Maneta, M., Anderegg, W. R. L., Martinez-Vilalta, J., & Sala, A. (2019). Plant water content integrates hydraulics and carbon depletion to predict drought-induced seedling mortality. *Tree Physiology*. https://doi.org/10.1093/treephys/tpz062

Serbin, S. P., Singh, A., McNeil, B. E., Kingdon, C. C., & Townsend, P. A. (2014). Spectroscopic determination of leaf morphological and biochemical traits for northern temperate and boreal tree species. *Ecological Applications*. https://doi.org/10.1890/13-2110.1

Sevanto, S., Mcdowell, N. G., Dickman, L. T., Pangle, R., & Pockman, W. T. (2014). How do trees die? A test of the hydraulic failure and carbon starvation hypotheses. *Plant, Cell and Environment*. https://doi.org/10.1111/pce.12141

Swinfield, T., Both, S., Riutta, T., Bongalov, B., Elias, D., Majalap-Lee, N., et al. (2019). Imaging spectroscopy reveals the effects of topography and logging on the leaf chemistry of tropical forest canopy trees. *Global Change Biology*, *n/a*(n/a). https://doi.org/10.1111/gcb.14903

Thirumalai, K., DInezio, P. N., Okumura, Y., & Deser, C. (2017). Extreme temperatures in Southeast Asia caused by El Ninõ and worsened by global warming. *Nature Communications*. https://doi.org/10.1038/ncomms15531

Ustin, S. L., Asner, G. P., Gamon, J. A., Fred Huemmrich, K., Jacquemoud, S., Schaepman, M., & Zarco-Tejada, P. (2006). Retrieval of quantitative and qualitative information about plant pigment systems from high resolution spectroscopy. In *International Geoscience and Remote Sensing Symposium (IGARSS)*. https://doi.org/10.1109/IGARSS.2006.517

Ustin, S. L., Gitelson, A. A., Jacquemoud, S., Schaepman, M., Asner, G. P., Gamon, J. A., & Zarco-Tejada, P. (2009). Retrieval of foliar information about plant pigment systems from high resolution spectroscopy. *Remote Sensing of Environment*. https://doi.org/10.1016/j.rse.2008.10.019

Walsh, R. P. D., & Newbery, D. M. (1999). The ecoclimatology of Danum, Sabah, in the context of the world's rainforest regions, with particular reference to dry periods and their impact. *Philosophical Transactions of the Royal Society B: Biological Sciences*. https://doi.org/10.1098/rstb.1999.0528

Wright, I. J., Reich, P. B., Westoby, M., Ackerly, D. D., Baruch, Z., Bongers, F., et al. (2004). The worldwide leaf economics spectrum. *Nature*. https://doi.org/10.1038/nature02403

Wright, S. J., Kitajima, K., Kraft, N. J. B., Reich, P. B., Wright, I. J., Bunker, D. E., et al. (2010). Functional traits and the growth-mortality trade-off in tropical trees. *Ecology*. https://doi.org/10.1890/09-2335.1

Wu, J., Kobayashi, H., Stark, S. C., Meng, R., Guan, K., Tran, N. N., et al. (2018). Biological processes dominate seasonality of remotely sensed canopy greenness in an Amazon evergreen forest. *New Phytologist*. https://doi.org/10.1111/nph.14939

Zanne, A. E., Westoby, M., Falster, D. S., Ackerly, D. D., Loarie, S. R., Arnold, S. E. J., & Coomes, D. A. (2010). Angiosperm wood structure: Global patterns in vessel anatomy and their relation to wood density and potential conductivity. *American Journal of Botany*. https://doi.org/10.3732/ajb.0900178